

SCIENTIFIC REPORTS



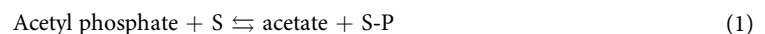
OPEN

Investigation of pyrophosphate versus ATP substrate selection in the *Entamoeba histolytica* acetate kinase

Thanh Dang & Cheryl Ingram-Smith

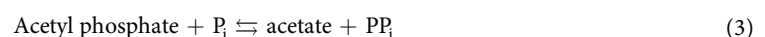
Acetate kinase (ACK; E.C. 2.7.2.1), which catalyzes the interconversion of acetate and acetyl phosphate, is nearly ubiquitous in bacteria but is present only in one genus of archaea and certain eukaryotic microbes. All ACKs utilize ATP/ADP as the phosphoryl donor/acceptor in the respective directions of the reaction (acetate + ATP \rightleftharpoons acetyl phosphate + ADP), with the exception of the *Entamoeba histolytica* ACK (EhACK) which uses pyrophosphate (PP_i)/inorganic phosphate (P_i) (acetyl phosphate + P_i \rightleftharpoons acetate + PP_i). Structural analysis and modeling of EhACK indicated steric hindrance by active site residues constricts entry to the adenosine pocket as compared to ATP-utilizing *Methanosarcina thermophila* ACK (MtACK). Reciprocal alterations were made to enlarge the adenosine pocket of EhACK and reduce that of MtACK. The EhACK variants showed a step-wise increase in ADP and ATP binding but were still unable to use these as substrates, and enzymatic activity with P_i/PP_i was negatively impacted. Consistent with this, ATP utilization by MtACK variants was negatively affected but the alterations were not sufficient to convert this enzyme to P_i/PP_i utilization. Our results suggest that controlling access to the adenosine pocket can contribute to substrate specificity but is not the sole determinant.

Acetate kinase (ACK; E.C. 2.7.2.1) catalyzes the reversible transfer of phosphate from acetyl phosphate to a phosphoryl acceptor (S), yielding acetate and a phosphorylated product (S-P) [Eq. 1]. ACK, nearly ubiquitous in bacteria, has been identified in just a single genus of archaea, *Methanosarcina*. In recent years, ACK has also been identified in certain eukaryotic microbes including the green algae *Chlamydomonas*, eucaryote and basidiomycete fungi, and certain protists, namely *Entamoeba histolytica*¹.



This enzyme was discovered in 1944² and the first kinetic characterization was reported in 1954³. In 2001, Buss *et al.* solved the structure for the *Methanosarcina thermophila* ACK (MtACK), and subsequent studies with this archaeal enzyme determined that ACK proceeds through a direct in-line mechanism of phosphoryl transfer⁴⁻⁶. Acyl substrate selection in ACK has been studied in the *Methanosarcina* enzyme. Four key residues, Val⁹³, Leu¹²², Phe¹⁷⁹, and Pro²³², have been shown to form a hydrophobic pocket for acetate binding⁷ implicated in acyl substrate selection in this enzyme. In particular, Val⁹³ appears to play an important role in limiting substrate length.

Ordinarily, ACK utilizes ATP/ADP as phosphoryl donor/acceptor; however, the *E. histolytica* enzyme is unusual in that it is PP_i-dependent. Instead of using ATP/ADP as the phosphoryl donor/acceptor [Eq. 2], *E. histolytica* ACK (EhACK) can only use pyrophosphate (PP_i)/inorganic phosphate (P_i) as the phosphoryl donor/acceptor [Eq. 3]⁸⁻¹⁰.



Department of Genetics and Biochemistry and the Eukaryotic Pathogens Innovation Center, Clemson University, Clemson, SC, 29634, USA. Correspondence and requests for materials should be addressed to C.I.-S. (email: cheryli@clemson.edu)

whereas most ATP-dependent ACKs function in both directions of the reaction, the *E. histolytica* enzyme strongly prefers the acetate-forming direction^{8–10}. Double reciprocal plots of substrate concentration versus enzyme activity indicated EhACK follows a ternary-complex mechanism^{8–10}, supporting a direct in-line mechanism of phosphoryl transfer as seen for MtACK^{4–6}. Currently, EhACK is the only known ACK to utilize pyrophosphate or inorganic phosphate as a phosphoryl donor or acceptor instead of ATP.

ACK belongs to the ASKHA (acetate, sugar kinase, heat shock and actin) enzyme superfamily. In 1992, Bork *et al.* identified PHOSPHATE1, PHOSPHATE2 and ADENOSINE as three signature ATPase motifs shared by members of this superfamily¹¹. These three conserved motifs form part of the adenosine binding pocket and are directly involved in ATP binding. Thaker *et al.* solved the EhACK structure and noted two amino acids substitutions in the ADENOSINE motif versus MtACK that may sterically hinder ATP binding¹².

Here, we investigated the role of residues in the ADENOSINE and PHOSPHATE2 motifs in phosphoryl substrate selection and utilization in ACK. Our results indicated that the adenosine pocket and the ADENOSINE motif play a critical role in ATP binding. However, ATP binding alone did not lead to utilization. Thus, although EhACK shares strong similarities with ATP-dependent ACKs, subtle differences have dramatically shaped its identity and function.

Results

Structures have been solved for six bacterial (four of which are from *Mycobacterium*), one archaeal, and two eukaryotic ACKs^{4, 12–14}. Although the global structures are similar, the percent identity and similarity between these ACK sequences showed that the eukaryotic ACKs are less related to the bacterial and archaeal enzymes (Supplemental Table S1). Previous phylogenetic analysis revealed that fungal ACKs belong to a distinct clade but the *E. histolytica* and other eukaryotic sequences group with the bacterial and archaeal ACKs¹. Thus, the unique P_i/PP_i-dependence of EhACK must be due to localized differences in the active site.

Structural differences between the adenosine binding pocket of PP_i-and ATP-ACKs. In addition to the PHOSPHATE1, PHOSPHATE2, and ADENOSINE sequence motifs, Ingram-Smith *et al.*¹⁵ defined two other regions designated as LOOP3 and LOOP4 that also influence ATP binding in ACK. Inspection of the active site in the MtACK structure showed that these regions surround the ATP binding site, with ADENOSINE forming a hydrophobic pocket for the adenosine moiety of ADP/ATP^{4, 7, 10, 12, 15}. ConSurf analysis (<http://consurf.tau.ac.il>), which estimates the evolutionary conservation at each position based on phylogenetic and structural analysis, indicated that the central positions in ADENOSINE have the highest conservation level (Fig. 1). Positions 322–327 of EhACK are of particular note as this region of the ADENOSINE motif is strongly conserved in other ACKs but not EhACK.

ADP/ATP-utilizing ACKs have a highly conserved Gly residue and an adjacent Ile/Val within the ADENOSINE motif (positions 331 and 332 in MtACK). Inspection of the MtACK structure revealed a large opening to the adenosine binding pocket (Fig. 2A) that is also evident in the structures of other ATP-ACKs. Occlusion of the adenosine pocket is evident in the surface representation of EhACK (Fig. 2B). Thaker *et al.*¹² postulated that Gln³²³Met³²⁴ within the ADENOSINE motif of EhACK may sterically prevent ADP/ATP binding.

Role of the ADENOSINE motif in ATP/ADP versus PP_i/P_i utilization. To investigate the role of the ADENOSINE motif in determining substrate selection, EhACK variants were created that simulate the open adenosine pocket observed in ATP-dependent ACKs. Gln³²³ and Met³²⁴ were altered to Gly and Ile, respectively, to mimic the residues found at equivalent positions in MtACK. These positions were also both altered to Ala to minimize side chain intrusions into the opening of the adenosine pocket. The reverse alterations were made in MtACK, converting Gly³³¹-Ile³³² to Gln-Met, respectively, to determine the effect of closing the entry to the adenosine pocket. The EhACK and MtACK variants were purified (Supplemental Figure S1) and kinetic parameters were determined in both directions of the reaction (Table 1).

The Q³²³G-M³²⁴I and Q³²³A-M³²⁴A EhACK variants displayed similar K_m values for acetyl phosphate and slightly decreased K_m values for phosphate as the unaltered enzyme but the k_{cat} values were decreased 8.3-fold for the Q³²³G-M³²⁴I variant and 19-fold for Q³²³A-M³²⁴A variant, resulting in ~7 and 11-fold reduced catalytic efficiency, respectively. In the direction of acetyl phosphate formation, these variants displayed slightly increased K_m for acetate but no increase in K_m for PP_i and only mild decrease in k_{cat} . No activity was observed with either variant using ATP or ADP as substrate in the respective direction of the reaction.

The G³³¹Q-I³³²M alteration in MtACK resulted in substantial reductions in k_{cat} (Table 1). In the acetate-forming direction, catalysis was reduced over 100-fold, and in the acetyl phosphate-forming direction, k_{cat} was reduced ~50-fold. This alteration resulted in ~5-fold increase in K_m for ADP and ATP, and a 15-fold increase in K_m for acetate but no substantial change in the K_m for acetyl phosphate. As for wild-type MtACK, no activity was observed with P_i or PP_i as substrate in the respective directions of the reaction.

Additional structural elements may contribute to occlusion of the ATP/ADP binding pocket. A salt bridge between Arg²⁷⁴ and Asp²⁷² on LOOP4 of EhACK may cause further constriction of the adenosine pocket by positioning the Arg side chain in toward the pocket¹². These two residues are conserved in MtACK but the side chain of Arg is positioned away from the adenosine pocket. These residues are not conserved in among all ACKs though and LOOP4 does not impinge upon the adenosine pocket. The PHOSPHATE2 motif, which interacts with the β phosphate of ATP and was suggested to have a role in substrate positioning^{4, 11, 15}, is longer in EhACK and protrudes farther into the active site than in the ATP-dependent enzymes (Fig. 2C). Sequence alignment and structural superposition of the PHOSPHATE 2 motif illustrate that this difference arises from addition of a single residue, Gly²⁰³ (Figs 1 and 2D).

PHOSPHATE2			
Ehist	193	KIIACHLGTGGSSCCGIV	210
Mtherm	203	KIITCHLNG-SSITAVE	219
Cneo	215	NVVVAHLGSG-SSSCCIK	231
Styph	205	NIITCHLNG-GSVSAIR	221
Tmari	202	KIITCHIGNG-ASVAAVK	218
Msmeg	184	NQIVLHLGNG-ASASAVA	200
Mavium	192	KQIVLHLGNG-CSASAIA	208
Mpara	192	KQIVLHLGNG-CSASAIA	208
Mmari	192	NQIVLHLGNG-ASASAVA	208
		: . . * : * . * * :	
CONSURF		857879899696923951	
ADENOSINE			
Ehist	317	LLVFTD <u>Q</u> MGLEVWQVRKA	334
Mtherm	325	AVVFTA <u>G</u> I GENSASIRKR	342
Cneo	355	GLVFSG <u>G</u> I GEKGAELRRD	372
Styph	327	AVVFTG <u>G</u> I GENAAMVREL	344
Tmari	325	AIVFTA <u>G</u> V GENSPITRED	342
Msmeg	305	VISFTA <u>G</u> V GENVPPVRRD	322
Mavium	313	VISFTA <u>G</u> I GENDA AVR RD	330
Mpara	313	VISFTA <u>G</u> I GENDA AVR RD	330
Mmari	313	VVSFTA <u>G</u> I GEHDA AVR RD	330
		: * : : * . * . *	
CONSURF		456998969996111911	

Figure 1. Partial alignment of ACK amino acid sequences. Sequences of ACKs for which the structure have been solved were aligned and ConSurf analysis was performed to examine sequence conservation. The PHOSPHATE2 and ADENOSINE motifs are shown. The full alignment is provided in the Supplemental Information (Supplemental Figure S2). Abbreviations and PDB accession numbers: Ehist, *E. histolytica*, PDB ID 4H0O; *Methanosarcina thermophila*, PDB ID 1TUY; Cneo, *Cryptococcus neoformans*, PDB ID 4H0P; Styph, *Salmonella typhimurium*, PDB ID 3SLC; Tmari, *Thermotoga maritima*, PDB ID 2IIR; Msmeg, *Mycobacterium smegmatis*, PDB ID 4IJN; Mavium, *Mycobacterium avium*, PDB ID 3P4I; Mpara, *Mycobacterium paratuberculosis*, PDB ID 3R9P; Mmari, *Mycobacterium marinum* PDB ID 4DQ8.

To examine whether this salt bridge and the extended PHOSPHATE2 motif influence substrate selection, EhACK Q³²³G-M³²⁴I variants in which the salt bridge has been eliminated (D²⁷²A-R²⁷⁴A-Q³²³G-M³²⁴I) or in which the PHOSPHATE2 motif has been shortened (Δ G²⁰³-Q³²³G-M³²⁴I) were analyzed. The D²⁷²A-R²⁷⁴A-Q³²³G-M³²⁴I replacement decreased k_{cat} in the acetate-forming direction by ~2,500–5,000 fold but had little effect on K_m for either substrate (Table 1). This variant had no detectable activity in the acetyl phosphate-forming direction (Table 1). The Δ G²⁰³-Q³²³G-M³²⁴I variant was inactive in either direction of the reaction, and thus the effect of the Gly²⁰³ deletion compounded onto the D²⁷²A-R²⁷⁴A-Q³²³G-M³²⁴I alteration was not examined. No enzymatic activity was observed with either of these variants using ATP or ADP as the substrate in place of PP_i or P_i.

Inhibition of EhACK and MtACK by alternative phosphoryl donors and acceptors. Since wild-type EhACK and MtACK cannot utilize ATP/ADP or PP_i/P_i, respectively, as alternative phosphoryl donor/acceptor, inhibition assays were performed to determine whether these compounds can bind and inhibit activity even if they cannot be used productively as substrate. EhACK activity was measured in the favored acetate-forming direction in the presence or absence of 10 mM AMP, ADP, or ATP (Fig. 3A). Although AMP had no effect, both ADP and ATP were found to inhibit EhACK activity but to differing extents. The presence of ATP resulted in nearly 80% inhibition versus ~30% inhibition by ADP. The presence of P_i or PP_i with AMP was not sufficient to mimic the effect of inhibition by ADP or ATP, respectively (data not shown). For MtACK, P_i had no effect on enzymatic activity. PP_i inhibited the enzyme in both directions of the reaction to differing extents, producing ~70% inhibition in the acetate-forming direction and ~90% inhibition in the acetyl phosphate-forming direction (Fig. 3B and C).

The mode of inhibition of EhACK by ATP was determined by kinetic analysis using a matrix of reactions in which the ATP concentration was varied versus P_i concentration with the acetate concentration held constant. ATP was found to be a competitive inhibitor of EhACK, as demonstrated by the results in Fig. 4. Further examination of ATP inhibition of the EhACK variants in the favored acetate-forming direction of the reaction revealed that a similar final level of inhibition of ~85–90% was achieved for the variants and wild-type enzyme by 15 mM ATP (Fig. 5A).

The IC₅₀ value for ATP, defined as the concentration of ATP required to cause 50% inhibition of enzymatic activity, was reduced for the EhACK variants versus the wild-type enzyme (Table 2). The IC₅₀ values were reduced

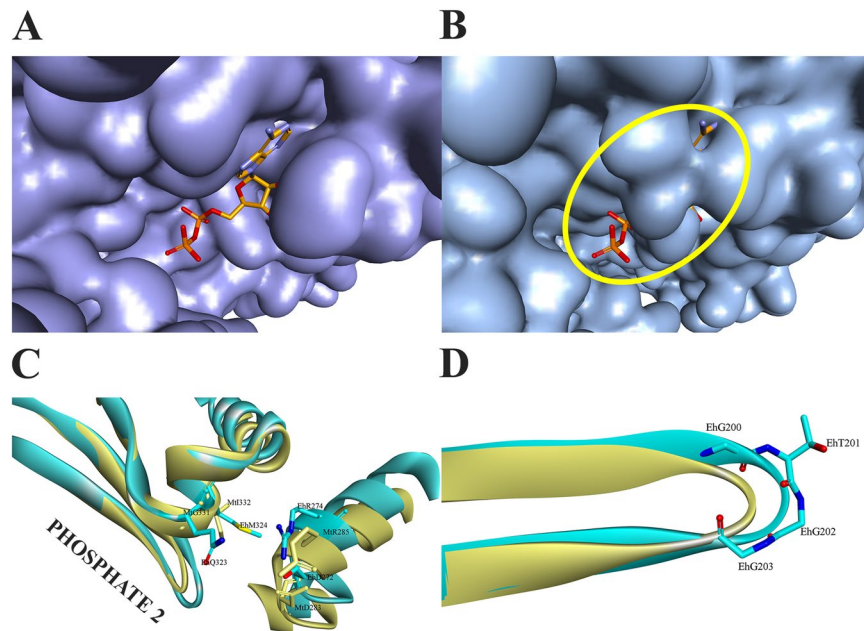


Figure 2. The ACK adenosine binding pocket. **(A)** Surface representation of MtACK with bound ADP. **(B)** Surface representation of EhACK. The constricted opening to the adenosine pocket is circled. The position of bound ADP in MtACK was superimposed into the EhACK structure. **(C)** Superimposition of the adenosine pocket from MtACK (yellow) and EhACK (cyan) showing the positions of targeted residues. **(D)** Superimposed PHOSPHATE2 motifs from MtACK (yellow) and EhACK (cyan), showing the position of the additional Gly in the EhACK PHOSPHATE2 motif.

20–30% for the two Q³²³-M³²⁴ variants versus the wild-type enzyme, whereas the quadruple variant in which both the Q³²³-M³²⁴ residues and the D²⁷²-R²⁷⁴ salt bridge were altered had an IC₅₀ value that was reduced by over 60%. Since ATP is a competitive inhibitor of EhACK activity, this increase in inhibition suggests that the D²⁷²A-R²⁷⁴A-Q³²³G-M³²⁴I variant binds ATP more efficiently than wild-type enzyme even though it cannot use it as a substrate.

For MtACK, inhibition by PP_i in the acetate-forming direction was similar for the wild-type enzyme and the G³³¹Q-I³³²M variant, with ~70% maximum inhibition observed (Fig. 5B). The IC₅₀ values for PP_i were similar for both enzymes (Table 2). PP_i inhibition in the acetyl phosphate-forming direction was much stronger, reaching greater than 90% for both the wild-type and variant enzymes. However, maximum inhibition for the wild-type enzyme was achieved at lower ATP concentration (20–25 mM versus 40 mM for the variant). This is reflected in the IC₅₀ value, which is nearly two-fold higher for the G³³¹Q-I³³²M variant than for the wild-type.

Discussion

Substrate selection in ATP-utilizing ACKs. Thaker *et al.*¹², in analysis of the MtACK and EhACK structures, predicted that P_i/PP_i binding does not involve the adenosine pocket and PP_i likely binds in a position corresponding to the position of the β- and γ-phosphates of ATP in MtACK. Our inspection of structures for the four *Mycobacterium* ACKs and the *S. enterica* ACKs in addition to those for MtACK and *C. neoformans* ACK showed that the opening to the adenosine pocket is not occluded in ATP-utilizing ACKs, only in the EhACK structure. Thus, we investigated whether phosphoryl donor selection by ACK is based primarily on accessibility of the adenosine pocket.

Alterations were made to MtACK to determine if the substrate specificity could be changed from ATP to PP_i if the adenosine pocket was occluded. Catalysis was greatly reduced (~50–150 fold) in the enzyme variants and this was accompanied by increases in the K_m values for both acetate and ATP in the acetyl phosphate-forming direction of the reaction. Gorrell *et al.*¹⁶, using tryptophan fluorescence quenching, found that domain closure occurs upon nucleotide binding. Thus, the effects of these alterations on MtACK activity may be complicated to interpret as reduced catalysis could be due to inefficient utilization of ATP and to an influence in domain closure. Notably though, substrate specificity did not change and the MtACK variant was unable to utilize PP_i as a substrate. Thus, conversion of ATP-dependent MtACK to a P_i/PP_i-dependent enzyme could not be achieved by simple closure of the adenosine pocket.

MtACK has a broad NTP substrate range^{15, 17} with a preference for ATP and is highly active in both the acetate- and acetyl phosphate-forming directions. Ingram-Smith *et al.*¹⁵ examined the roles of conserved active site residues in NTP substrate selection in MtACK, and found that Gly³³¹ in the ADENOSINE motif exerted a strong influence. Asn²¹¹ in the PHOSPHATE2 motif and Gly²³⁹ in the LOOP3 motif were found to be important for enzymatic activity but did not play a substantial role in NTP preference.

Enzyme	Substrate	K_m (mM)	k_{cat} (sec ⁻¹)	k_{cat}/K_m (sec ⁻¹ mM ⁻¹)
EhACK				
Acetate-forming direction				
Wild-type	AcP	0.57 ± 0.03	266 ± 12	467 ± 44
Q ³²³ G-M ³²⁴ I		0.47 ± 0.04	32 ± 1.0	68 ± 7.5
Q ³²³ A-M ³²⁴ A		0.34 ± 0.07	14 ± 1.2	42 ± 5.3
G ²⁰³ deletion-Q ³²³ G-M ³²⁴ I		No detectable activity		
D ²⁷² A-R ²⁷⁴ A-Q ³²³ G-M ³²⁴ I		0.66 ± 0.11	0.052 ± 0.005	0.08 ± 0.01
Wild-type	P _i	14 ± 1.2	196 ± 5	14 ± 1.7
Q ³²³ G-M ³²⁴ I		7.3 ± 0.5	28 ± 1.2	3.8 ± 0.35
Q ³²³ A-M ³²⁴ A		8.2 ± 1.1	20 ± 0.8	2.5 ± 0.22
G ²⁰³ deletion-Q ³²³ G-M ³²⁴ I		No detectable activity		
D ²⁷² A-R ²⁷⁴ A-Q ³²³ G-M ³²⁴ I		18 ± 1.2	0.076 ± 0.004	0.004 ± 0.0002
Acetyl phosphate-forming direction				
Wild-type	Acetate	166 ± 7	1.4 ± 0.05	0.0086 ± 0.0004
Q ³²³ G-M ³²⁴ I		372 ± 40	0.51 ± 0.02	0.0014 ± 0.0001
Q ³²³ A-M ³²⁴ A		566 ± 44	0.51 ± 0.03	0.0009 ± 0.0001
G ²⁰³ deletion-Q ³²³ G-M ³²⁴ I		No detectable activity		
D ²⁷² A-R ²⁷⁴ A-Q ³²³ G-M ³²⁴ I		No detectable activity		
Wild-type	PP _i	2.1 ± 0.33	0.90 ± 0.03	0.44 ± 0.060
Q ³²³ G-M ³²⁴ I		2.0 ± 0.37	0.45 ± 0.03	0.23 ± 0.030
Q ³²³ A-M ³²⁴ A		2.3 ± 0.41	0.36 ± 0.01	0.16 ± 0.033
G ²⁰³ deletion-Q ³²³ G-M ³²⁴ I		No detectable activity		
D ²⁷² A-R ²⁷⁴ A-Q ³²³ G-M ³²⁴ I		No detectable activity		
MtACK				
Acetate-forming direction				
Wild-type	AcP	1.2 ± 0.09	1550 ± 54	1294 ± 56
G ³³¹ Q-I ³³² M		1.7 ± 0.14	12 ± 0.7	7.2 ± 0.16
Wild-type	ADP	1.8 ± 0.13	1915 ± 15	1073 ± 69
G ³³¹ Q-I ³³² M		5.7 ± 0.56	12 ± 0.5	2.0 ± 0.14
Acetyl phosphate-forming direction				
Wild-type	Acetate	20 ± 0.3	789 ± 16	39 ± 1.0
G ³³¹ Q-I ³³² M		302 ± 11	17 ± 4.2	0.057 ± 0.016
Wild-type	ATP	1.7 ± 0.03	711 ± 23	421 ± 10
G ³³¹ Q-I ³³² M		9.4 ± 0.27	14 ± 0.2	1.5 ± 0.054

Table 1. Apparent kinetic parameters for wild-type and variant EhACKs and MtACKs.

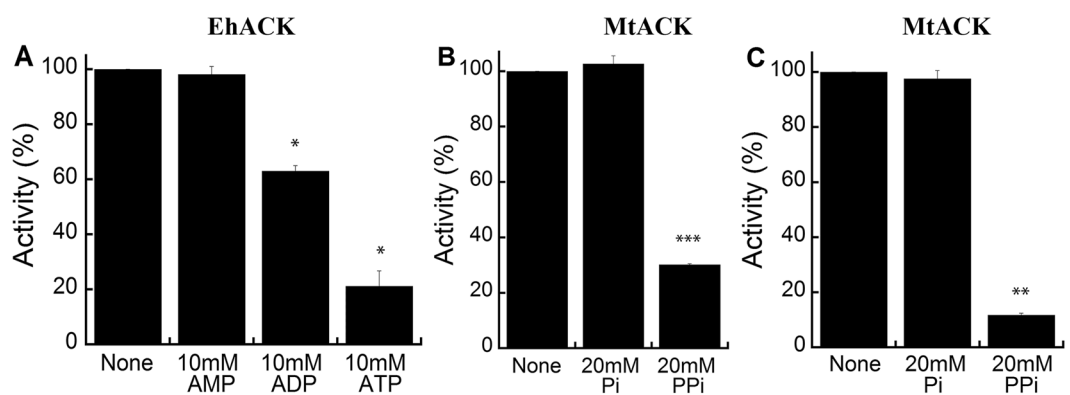


Figure 3. Inhibition of EhACK and MtACK by alternative phosphoryl donors and acceptors. (A) Inhibition of wild-type EhACK in the presence of 10 mM AMP, ADP, or ATP in the acetate-forming direction of the reaction. (B) Inhibition of wild-type MtACK in the presence of 20 mM P_i or PP_i in the acetate-forming direction. (C) Inhibition of wild-type MtACK in the presence of 20 mM P_i or PP_i in the acetyl phosphate-forming direction. Significant difference between inhibitions compared to wild-type enzyme activity is tested using an unpaired Welch t-test with R. *p-value < 0.001, **p-value < 0.00003, ***p-value < 0.000008. Activities are the mean ± SD of three replicates.

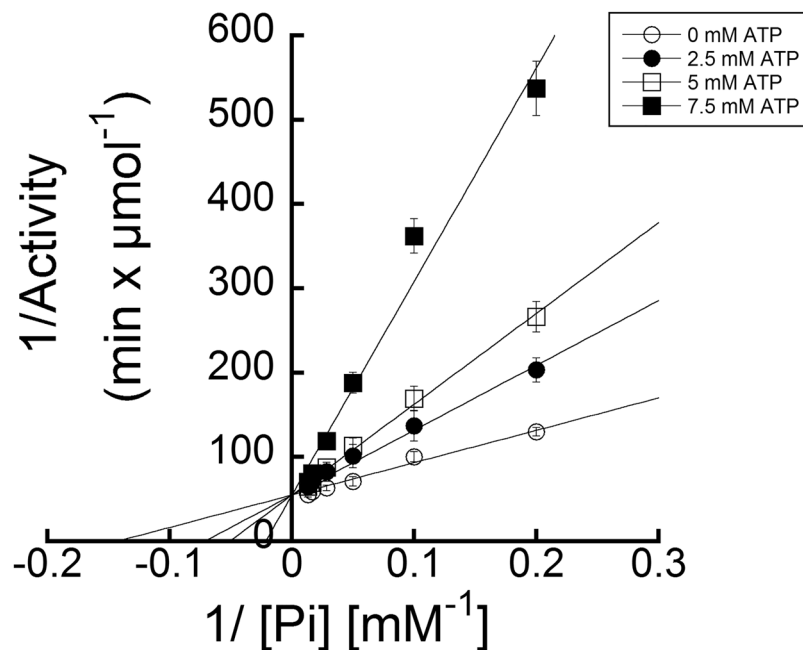


Figure 4. ATP is a competitive inhibitor of EhACK. Double reciprocal plot of EhACK activity versus P_i concentration in the absence (○) or presence of 2.5 mM (●), 5 mM (□), or 7.5 mM ATP (■). Activities are the mean \pm SD of three replicates.

Yoshioka *et al.*¹⁰ studied four residues in the ADENOSINE motif and one residue in the PHOSPHATE2 motif of *E. coli* ACK for their role in ATP versus PP_i substrate determination. The candidate residues Asn²¹³, Gly³³², Gly³³³, Ile³³⁴ and Asn³³⁷ were altered to the respective residues present in EhACK (Thr, Asp, Gln, Met, and Glu, respectively) and the ability of the enzyme variants to utilize PP_i in place of ATP was examined. All five variants displayed increased K_m for ATP and decreased catalysis but none was able to utilize PP_i .

Yoshioka *et al.*¹⁰ also examined the distribution of the *E. coli* ACK candidate residues and the corresponding residues in EhACK among 2625 ACK homologs. They suggested that Asn³³⁷ (Glu³²⁷ of EhACK) is most important in determining substrate selection as it is present in the ten ACK sequences most closely related to EhACK. However, their kinetic results with the Asn³³⁷ variants are inconclusive in this regard, although the kinetic results for this and other variants do strongly support a major role in ATP binding for the ADENOSINE motif but do not delineate specific residues responsible for determining ATP versus PP_i utilization.

Substrate selection in PP_i -dependent EhACK. As a converse to our experiments with MtACK, we altered residues blocking the opening to the adenosine pocket in EhACK to reduce the occlusion and evaluated the enzyme's ability to utilize P_i/PP_i versus ATP/ADP. The EhACK variants exhibited decreased activity with P_i and PP_i , much as we expected. Although catalysis was reduced for the Q³²³G-M³²⁴I and Q³²³A-M³²⁴A variants, further opening of the entrance to the adenosine pocket in the D²⁷²A-R²⁷⁴A-Q³²³G-M³²⁴I variant almost completely eliminated activity. This suggested that as the opening to the adenosine pocket increases, P_i and PP_i may still bind but their positioning may be suboptimal.

Although the enzyme variants were still unable to utilize ATP as a substrate, ATP and ADP did inhibit enzyme activity. The level of inhibition increased as the opening to the adenosine pocket was expanded, especially for the D²⁷²A-R²⁷⁴A-Q³²³G-M³²⁴I variant. This suggested that ATP and ADP could now enter the adenosine pocket and interfere with P_i binding. Such an interpretation of these results is supported by the observation that ATP inhibition is competitive versus P_i .

The similar behavior of the Q³²³G-M³²⁴I and Q³²³A-M³²⁴A variants with respect to inhibition by ATP indicated that the increased binding (as judged by IC_{50} values) must be due to expanding the entrance to the adenosine pocket rather than a specific interaction between the altered residues and ATP. Models of the enzyme variants indicated that these alterations to the adenosine pocket would result in decreased impairment of ATP binding (Fig. 6). In particular, deletion of G²⁰³ to shorten the PHOSPHATE2 loop combined with alteration of the ADENOSINE motif and removal of the D²⁷²-R²⁷⁴ salt bridge should allow the pocket to accommodate ATP well (Fig. 6C). Although the alterations made to EhACK appeared to increase the enzyme's ability to bind ATP, as indicated by the inhibition results, ATP was still not an effective substrate.

Other possible PP_i -dependent ACKs. Using a BLASTp search of the non-redundant protein sequence database at NCBI with EhACK as the query sequence, we identified a small number of putative ACK sequences that may also be PP_i -dependent or require a substrate other than ATP or PP_i . Several of these putative ACK sequences came from metagenome analyses of anaerobic digestors. However, there were four putative ACK deduced amino acid sequences that came from draft genomes for the bacteria *Ornatilinea apprima*, *Longilinea*

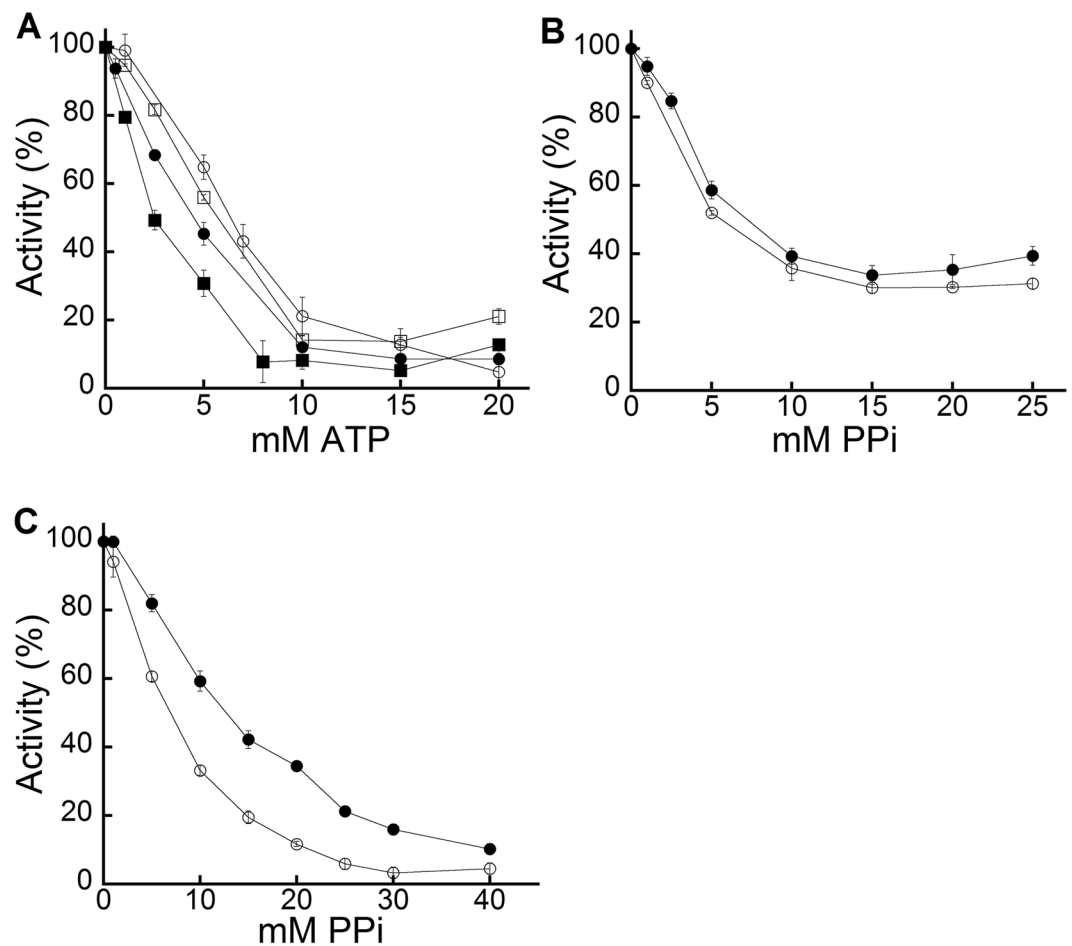


Figure 5. Inhibition curves for EhACK and MtACK wild-type and variant enzymes. Enzymatic activity was determined for each enzyme in the presence of the indicated concentration of ATP or PP_i. Activities were plotted as a percentage of the activity observed for the wild-type enzyme in the absence of inhibitor. Activities are the mean ± SD of three replicates. (A) ATP inhibition of EhACK and its variants in the acetate-forming direction. EhACK wild-type, (○); EhACK Q³²³G-M³²⁴I variant (●); EhACK Q³²³A-M³²⁴A variant, (□); EhACK D²⁷²A-R²⁷⁴A-Q³²³G-M³²⁴I variant (■). (B and C) PP_i inhibition of MtACK and its variants in the acetate-forming (B) and acetyl phosphate-forming (C) directions. MtACK wild-type, (○); MtACK G³³¹Q-I³³²M variant (●).

EhACK	ATP IC ₅₀ (mM)	
	Acetate-forming direction	
Wild-type	6.1 ± 0.05	
Q ³²³ G-M ³²⁴ I	4.2 ± 0.30	
Q ³²³ A-M ³²⁴ A	4.8 ± 0.09	
D ²⁷² A-R ²⁷⁴ A-Q ³²³ G-M ³²⁴ I	2.4 ± 0.19	
MtACK	PP _i IC ₅₀ (mM)	
	Acetate-forming direction	Acetyl phosphate-forming direction
	Wild-type	7.5 ± 0.28
G ³³¹ Q-I ³³² M	4.0 ± 0.28	14 ± 1.1

Table 2. IC₅₀ values for ATP inhibition of EhACK and PP_i inhibition of MtACK. ND, not determined because the enzyme was inactive in this direction.

arvoryae, *Flexilinea flocculi*, and *Leptolinea tardivitalis*^{18–21}. These bacteria are all obligate anaerobes from the phylum *Chloroflexi* within the family *Anaerolineaceae*. Three of the four produce acetate as a main product from glucose fermentation; *L. arvoryae* also produces acetate as a primary fermentation product but from growth

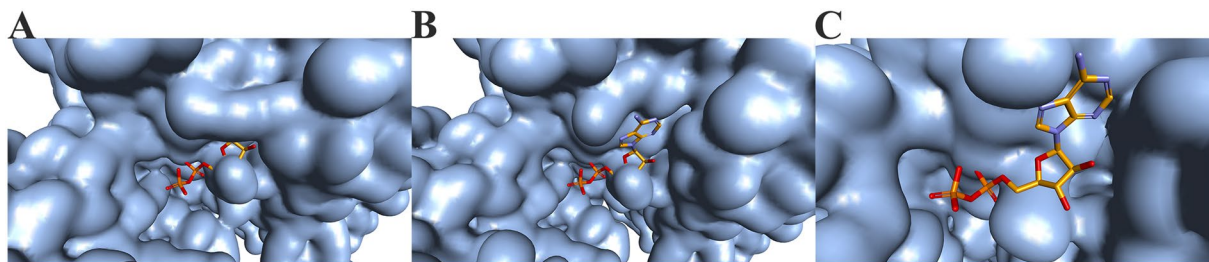


Figure 6. *In silico* modeling of the adenosine binding pocket of EhACK variants. Models were built using Accelrys Discovery Studio version 3.5 (Biovia). ADP binding in MtACK was superimposed into the EhACK structure models. (A) Q³²³G-M³²⁴I variant. (B) D²⁷²A-R²⁷⁴A-Q³²³G-M³²⁴I variant. (C) ΔG²⁰³-D²⁷²A-R²⁷⁴A-Q³²³G-M³²⁴I variant.

		PHOSPHATE2			
Ehis	193	KIIACHLGTG	G SSCCGIV	210	
Enut	193	KIIACHLGTG	G SSCCGIV	210	
Edis	193	KIIACHLGTG	G SSCCGIV	210	
Ein	193	KIVACHLGTG	G SSCCAIL	210	
Oapp	201	KIIACHLGTG	G S S A V A L K	218	
Larv	201	KLILCHLGTG	G S S V V A M K	218	
Fflo	201	KFILCHLGS	G S S I T A V R	218	
Ltar	201	KLILCHLGTG	G S S V T A M K	218	
		*	* * * *	* * * *	

		ADENOSINE			
Ehis	317	LLVFTD	Q MGLEVWQVRKA	334	
Enut	317	LLVFTD	Q MGLEVWQVRRRA	334	
Edis	317	LLVFTD	Q MGLEVWQVRKA	334	
Ein	317	MLVFTD	Q VGLEVPVRKA	334	
Oapp	322	ALIFTD	D I GL W S W Q L R E S	339	
Larv	323	AIVFTD	D VGLKSWKLRAK	340	
Fflo	323	AIVFTD	D I G E T S W K L R E K	340	
Ltar	323	AIVFTD	D VGLKSWKLREK	340	
		* * *	*	*	

Figure 7. Partial alignment of putative PP_i-ACK amino acid sequences. Sequences were aligned using Clustal Omega. The PHOSPHATE2 and ADENOSINE motifs are shown. The full alignment is provided in the Supplemental Information (Supplemental Figure S3). Abbreviations and sequence accession numbers: Ehis, *E. histolytica*, XP_655990.1; Enut, *Entamoeba nuttalli*, XP_008860710.1; Edis, *Entamoeba dispar*, XP_001741606.1; Ein, *Entamoeba invadens*, XP_004254504.1; Oapp, *Ornatilinea apprima*, WP_075061087.1; Larv, *Longilinea arvoryzae*, WP_075074878.1; Fflo, *Flexilinea flocculi*, WP_062279690.1; Ltar, *Leptolinea tardivitalis*, WP_062422928.1.

on sucrose instead of glucose. Little else is known about these bacteria beyond their initial characterization for recognition as new species.

Alignment of these putative ACK sequences with those of the four *Entamoeba* ACK sequences (those from *E. histolytica*, *Entamoeba nuttalli*, *Entamoeba dispar*, and *Entamoeba invadens*) revealed two key findings. Within the PHOSPHATE2 motif, all eight of these sequences have the extended loop containing the second Gly residue (Fig. 7). These are the only putative ACK sequences identified to have this extended PHOSPHATE2 loop (see Supplemental Figure S1 for comparison). Within the ADENOSINE motif, all of these sequences have a conserved Asp residue (immediately adjacent to Q³²³-M³²⁴ of EhACK) that is not conserved in any other ACK sequences (all of which have Ala or Gly at the equivalent position, as shown in Fig. 1). Interestingly, these bacterial ACKs have a conserved Asp at the equivalent position to Gln³²³ of PP_i-dependent EhACK and the other *Entamoeba* ACKs. A completely conserved Gly resides at this position (Gly³³¹ of MtACK) in all ATP-dependent ACKs. Whether this indicates that these enzymes are neither ATP-dependent nor PP_i-dependent, or whether there is some flexibility in the identity of the residue at this position in PP_i-dependent ACKs is unknown.

Conclusions

Our results demonstrate that phosphoryl donor specificity in ACK is mediated not just by access to the adenosine binding pocket but by other elements as well, as simple opening or occlusion of the entrance to this pocket was not sufficient to alter substrate specificity. This suggests that the active sites of the ADP/ATP-dependent and P_i/PP_i -dependent enzymes have evolved to optimize utilization of their preferred substrate at the expense of the ability to use alternative substrates, and thus better suit their biological function.

Materials and Methods

Materials. Chemicals were purchased from Sigma-Aldrich, VWR International, Gold Biotechnology, Fisher Scientific, and Life Technologies. Oligonucleotide primers were purchased from Integrated DNA Technologies.

Site-directed mutagenesis. Site-directed mutagenesis of the *E. histolytica* *ack* (*ehack*) and *M. thermophila* *ack* (*mtack*) genes was performed according to manufacturer's instructions with the QuikChange II kit (Agilent Technologies, CA, USA). The altered sequences were confirmed by sequencing at the Clemson University Genomics Institute. Mutagenesis primers used are shown in Supplemental Table S2.

Recombinant protein production. EhACK and its variants were produced in *Escherichia coli* strain YBS121 Δ *ack* Δ *pta* carrying the pREP4 plasmid containing the *lacI* gene and purified as described in Fowler *et al.*⁹. MtACK and its variants were produced in *E. coli* Rosetta2 (DE3) pLysS and purified as described in Fowler *et al.*⁹. Purified enzymes were dialyzed overnight in 25 mM Tris-HCl, 150 mM NaCl, and 10% glycerol (pH 7.4), aliquoted, and stored at -80°C . Recombinant enzymes were examined by SDS-PAGE and estimated to be greater than 95% pure. Protein concentration was measured by absorbance at 280 nm using Take3 micro-volume plate (Biotek, VT, USA).

Determination of kinetic parameters. Kinetic parameters for the EhACK enzymes were determined using the colorimetric hydroxamate assay for the acetyl phosphate-forming direction^{2,3,17} and the reverse modified hydroxamate assay^{9,22} for the acetate-forming direction as previously described⁹. In the acetyl phosphate-forming direction, activities for EhACK and its variants were assayed in a mixture containing 100 mM morpholinoethanesulfonic acid (pH 5.5), 5 mM MgCl_2 , and 600 mM hydroxylamine hydrochloride (pH 7.5) with varying concentrations of acetate and sodium pyrophosphate. Reactions were performed at 45°C . For the acetate-forming direction, kinetic parameters were determined in a mixture of 100 mM Tris-HCl (pH 7.0) and 10 mM MgCl_2 with varying concentrations of sodium phosphate and acetyl phosphate. Enzymatic reactions were performed at 37°C .

The acetyl phosphate produced (acetyl phosphate-forming direction) or remaining (acetate-forming direction) was reacted with hydroxylamine to produce acetyl hydroxamate, which was then converted to a ferric hydroxamate complex by reaction with an acidic ferric chloride solution, making the solution change from a yellow to brownish red color that can be detected spectrophotometrically at 540 nm. Acetyl phosphate formation or depletion was determined by measuring the absorbance at 540 nm with an Epoch microplate spectrophotometer (Biotek) and comparison to an acetyl phosphate standard curve. Kinetic data were fit to the Michaelis-Menten equation by nonlinear regression using KaleidaGraph (Synergy Software) for determination of apparent kinetic parameters.

Similarly, kinetic parameters for MtACK and its variants were determined using the hydroxamate assay^{2,3,17} and the reverse modified hydroxamate assay^{9,22} as previously described. In the acetate-forming direction, enzyme activities were determined in 100 mM Tris (pH 7.5) with varying concentrations of MgADP and acetyl phosphate. For the acetyl phosphate-forming direction, kinetic parameters were determined in 100 mM Tris (pH 7.5) and 600 mM hydroxylamine (pH 7.5) with varying concentrations of acetate and MgATP. Enzymatic reactions were performed at 37°C .

Determination of inhibition parameters. Inhibition of EhACK by ATP and ADP and of MtACK by PP_i was determined using the hydroxamate and reverse modified hydroxamate assays as described above. All inhibition assays were performed using substrates at their K_m concentrations, with the exception of acetyl phosphate which was used at a concentration of 2 mM for all reactions in the acetate-forming direction. The half maximal inhibitory concentrations (IC_{50} values) were determined using PRISM 5 (Graphpad Software). ATP's mode of inhibition of wild-type EhACK was determined by measuring enzymatic activity in the acetate forming direction in a four by seven matrix of varied ATP and P_i concentrations, with other substrate concentrations kept constant.

ACK sequence alignment, ConSurf analysis, and structural modeling. ACK sequences were obtained from NCBI. Accession numbers are as follows: *E. histolytica*, PDB ID 4H0O; *Methanosarcina thermophila*, PDB ID 1TUJ; *Cryptococcus neoformans*, PDB ID 4H0P; *Salmonella typhimurium*, PDB ID 3SLC; *Thermotoga maritima*, PDB ID 2IIR; *Mycobacterium smegmatis*, PDB ID 4IJN; *Mycobacterium avium*, PDB ID 3P4I; *Mycobacterium paratuberculosis*, PDB ID 3R9P; *Mycobacterium marinum* PDB ID 4DQ8. Sequences alignments were performed using Clustal Omega^{23–25}. ACK structures were downloaded from Protein Data Bank (PDB): 4H0O (*Entamoeba histolytica*), 1TUJ (*M. thermophila*), 4H0P (*C. neoformans*), and 3SLC (*S. typhimurium*). Structure superposition and modeling were performed using Accelrys Discovery Studio 3.5 (Biovia). ConSurf analysis^{26–28} (<http://consurf.tau.ac.il>) was used to examine evolutionary conservation of ACK sequence and identify amino acids likely to play important structural and functional roles.

References

- Ingram-Smith, C., Martin, S. R. & Smith, K. S. Acetate kinase: not just a bacterial enzyme. *Trends Microbiol.* **14**, 249–253 (2006).
- Lipmann, F. Enzymatic synthesis of acetyl phosphate. *J. Biol. Chem.* **155**, 55–70 (1944).
- Rose, I. A., Grunberg-Manago, M., Korey, S. R. & Ochoa, S. Enzymatic phosphorylation of acetate. *J. Biol. Chem.* **211**, 737–756 (1954).

4. Buss, K. A. *et al.* Urkinase: structure of acetate kinase, a member of the ASKHA superfamily of phosphotransferases. *J. Bacteriol.* **183**, 680–686 (2001).
5. Gorrell, A., Lawrence, S. H. & Ferry, J. G. Structural and kinetic analyses of arginine residues in the active site of the acetate kinase from *Methanosarcina thermophila*. *J. Biol. Chem.* **280**, 10731–10742 (2005).
6. Miles, R. D., Gorrell, A. & Ferry, J. G. Evidence for a transition state analog, MgADP-aluminum fluoride-acetate, in acetate kinase from *Methanosarcina thermophila*. *J. Biol. Chem.* **277**, 22547–22552 (2002).
7. Ingram-Smith, C. *et al.* Characterization of the acetate binding pocket in the *Methanosarcina thermophila* acetate kinase. *J. Bacteriol.* **187**, 2386–2394 (2005).
8. Reeves, R. E. & Guthrie, J. D. Acetate kinase (pyrophosphate). A fourth pyrophosphate-dependent kinase from *Entamoeba histolytica*. *Biochem. Biophys. Res. Commun.* **66**, 1389–1395 (1975).
9. Fowler, M. L., Ingram-Smith, C. & Smith, K. S. Novel pyrophosphate-forming acetate kinase from the protist *Entamoeba histolytica*. *Eukaryot. Cell* **11**, 1249–1256 (2012).
10. Yoshioka, A., Murata, K. & Kawai, S. Structural and mutational analysis of amino acid residues involved in ATP specificity of *Escherichia coli* acetate kinase. *J. Biosci. Bioeng.* **118**, 502–507 (2014).
11. Bork, P., Sander, C. & Valencia, A. An ATPase domain common to prokaryotic cell cycle proteins, sugar kinases, actin, and hsp70 heat shock proteins. *Proc. Natl. Acad. Sci. USA* **89**, 7290–7294 (1992).
12. Thaker, T. M. *et al.* Crystal structures of acetate kinases from the eukaryotic pathogens *Entamoeba histolytica* and *Cryptococcus neoformans*. *J. Struct. Biol.* **181**, 185–189 (2013).
13. Baugh, L. *et al.* Increasing the structural coverage of tuberculosis drug targets. *Tuberculosis (Edinb)* **95**, 142–148 (2015).
14. Chittori, S., Savithri, H. S. & Murthy, M. R. Structural and mechanistic investigations on *Salmonella typhimurium* acetate kinase (AckA): Identification of a putative ligand binding pocket at the dimeric interface. *BMC Struct. Biol.* **12**, 24 (2012).
15. Ingram-Smith, C. *et al.* The role of active site residues in atp binding and catalysis in the *Methanosarcina thermophila* acetate kinase. *Life (Basel)* **5**, 861–871 (2015).
16. Gorrell, A. & Ferry, J. G. Investigation of the *Methanosarcina thermophila* acetate kinase mechanism by fluorescence quenching. *Biochemistry* **46**, 14170–14176 (2007).
17. Aceti, D. J. & Ferry, J. G. Purification and characterization of acetate kinase from acetate-grown *Methanosarcina thermophila*. Evidence for regulation of synthesis. *J. Biol. Chem.* **263**, 15444–15448 (1988).
18. Yamada, T. *et al.* *Anaerolinea thermolimos* sp. nov., *Levilinea saccharolytica* gen. nov., sp. nov. and *Leptolinea tardivitalis* gen. nov., sp. nov., novel filamentous anaerobes, and description of the new classes *Anaerolineae* classis nov. and *Caldilineae* classis nov. in the bacterial phylum *Chloroflexi*. *Int. J. Syst. Evol. Microbiol.* **56**, 1331–1340 (2006).
19. Yamada, T. *et al.* *Bellilinea caldifistulae* gen. nov., sp. nov. and *Longilinea arvoryzae* gen. nov., sp. nov., strictly anaerobic, filamentous bacteria of the phylum *Chloroflexi* isolated from methanogenic propionate-degrading consortia. *Int. J. Syst. Evol. Microbiol.* **57**, 2299–2306 (2007).
20. Podosokorskaya, O. A., Bonch-Osmolovskaya, E. A., Novikov, A. A., Kolganova, T. V. & Kublanov, I. V. *Ornatilinea apprima* gen. nov., sp. nov., a cellulolytic representative of the class *Anaerolineae*. *Int. J. Syst. Evol. Microbiol.* **63**, 86–92 (2013).
21. Sun, L. *et al.* Isolation and characterization of *Flexilinea flocculi* gen. nov., sp. nov., a filamentous anaerobic bacterium belonging to the class *Anaerolineae* in the phylum *Chloroflexi*. *Int. J. Syst. Evol. Microbiol.* **66**, 988–996 (2015).
22. Fowler, M. L., Ingram-Smith, C. J. & Smith, K. S. Direct detection of the acetate-forming activity of the enzyme acetate kinase. *J. Vis. Exp.* **58**, e3474 (2011).
23. Sievers, F. *et al.* Fast, scalable generation of high-quality protein multiple sequence alignments using Clustal Omega. *Mol. Syst. Biol.* **7**, 539–539 (2011).
24. McWilliam, H. *et al.* Analysis tool web services from the EMBL-EBI. *Nucleic Acids Res.* **41**, W597–600 (2013).
25. Li, W. *et al.* The EMBL-EBI bioinformatics web and programmatic tools framework. *Nucleic Acids Res.* **43**, W580–584 (2015).
26. Armon, A., Graur, D. & Ben-Tal, N. ConSurf: An algorithmic tool for the identification of functional regions in proteins by surface mapping of phylogenetic information. *J. Mol. Biol.* **307**, 447–463 (2001).
27. Glaser, F. *et al.* ConSurf: Identification of functional regions in proteins by surface-mapping of phylogenetic information. *Bioinformatics* **19**, 163–164 (2003).
28. Landau, M. *et al.* ConSurf 2005: The projection of evolutionary conservation scores of residues on protein structures. *Nucleic Acids Res.* **33**, W299–302 (2005).

Acknowledgements

We thank Kerry Smith (Clemson University) for beneficial discussions regarding this work. This work was supported by a grant from the National Institutes of Health (R15GM114759) and Clemson University.

Author Contributions

C.I.S. conceived and supervised the work and co-wrote the manuscript. T.D. designed and performed the experiments, analyzed the data, interpreted the results, and co-wrote the manuscript. Both authors reviewed the results and approved the final version of the manuscript.

Additional Information

Supplementary information accompanies this paper at doi:10.1038/s41598-017-06156-5

Competing Interests: The authors declare that they have no competing interests.

Publisher's note: Springer Nature remains neutral with regard to jurisdictional claims in published maps and institutional affiliations.



Open Access This article is licensed under a Creative Commons Attribution 4.0 International License, which permits use, sharing, adaptation, distribution and reproduction in any medium or format, as long as you give appropriate credit to the original author(s) and the source, provide a link to the Creative Commons license, and indicate if changes were made. The images or other third party material in this article are included in the article's Creative Commons license, unless indicated otherwise in a credit line to the material. If material is not included in the article's Creative Commons license and your intended use is not permitted by statutory regulation or exceeds the permitted use, you will need to obtain permission directly from the copyright holder. To view a copy of this license, visit <http://creativecommons.org/licenses/by/4.0/>.

© The Author(s) 2017